Oral presentation | Turbulence simulation (DNS,LES,RANS)

Turbulence simulation(DNS,LES,RANS)-V

Fri. Jul 19, 2024 10:45 AM - 12:45 PM Room B

[13-B-04] Empirical Two-Layer Model for Predicting Near-Wall Diffusive Flux at High Schmidt or Prandtl Numbers

*Kin Wing Wong[1], Ignas Mickus[1], Dmitry Grishchenko[1], Pavel Kudinov[1] (1. Division of Nuclear Science and Engineering, KTH Royal Institute of Technology, 11428 Stockholm, Sweden)

Keywords: Wall Function, High Prandtl and Schimdt Number, Wall Boudned Turbulent Flows

Twelfth International Conference on Computational Fluid Dynamics (ICCFD12), Kobe, Japan, July 14-19, 2024

Empirical Two-Layer Model for Predicting Near-Wall Diffusive Flux at High Schmidt or Prandtl Numbers

Kin Wing Wong*, Ignas Mickus, Dmitry Grishchenko, Pavel Kudinov
*Corresponding author: kwwo@kth.se
Division of Nuclear Science and Engineering, KTH Royal Institute of Technology, Stockholm, Sweden

Abstract: This paper proposes an empirical correction to the eddy-viscosity-based wall model for passive scalars, utilizing a two-layer concept to address variability caused by the low-pass filtering phenomenon in turbulent flows with high Schmidt (Sc) and Prandtl (Pr) numbers. The model incorporates two von Kármán-like constants (k_{Re} and k_{Sc}) to decouple the effects of Sc and Re. These constants are derived from existing LES and DNS databases, making it the best-estimated wall model for high Sc conditions. Its accuracy surpasses well-adopted models such as the Jayatilleke P-function and Kader's correlation for considered high Sc ranges. Validation through turbulent mass transfer experiments demonstrates the efficacy of the two-layer model without requiring excessive refinement to $y^+ = 0.1$ to 0.3 to capture the diffusive layer. This paper shows that the model can be applied to coarse grid simulations for both hydrodynamic and passive scalar fields, or used with wall-refined grids for hydrodynamics (y^+ close to 1) while accurately capturing near-wall flux in under-resolved concentration or passive scalar fields; however, some precautions are discussed to retain the optimal accuracy of the model.

Keywords: High Schmidt Number, Turbulent Flows, Wall Model, Low-Pass Filtering

1 Introduction

Flow-accelerated corrosion and erosion (FACE) in heavy liquid metal (HLM) coolant is a significant design issue that requires careful consideration to ensure the reliability of structural components in lead-cooled fast reactors (LFRs). The SUNRISE WP5 project attempts to research on this critical issue by developing a computational approach to study the FACE phenomenon [1].

The modeling of flow-accelerated corrosion (FAC) requires a detailed investigation of species transport between the solid material and the liquid coolant. Thus, accurate modeling or resolving the transport flux of concentration species is crucial, especially under conditions of mass transport with very high Schmidt numbers (Sc). Based on the correlations for density, dynamic viscosity, and diffusivity provided in [2, 3], Figure 1 illustrates that the Sc number for iron (Fe) or nickel (Ni) can reach a maximum of approximately 900 at low temperatures (400°C). As the temperature increases, the Sc decreases to several hundreds. To extend the longevity of the pump impeller in the LFRs, it is crucial to operate at the lower end of the temperature range. Therefore, modeling the situation with Sc at the high end of the range is necessary.

The elevated Sc number in these ranges results in the development of an ultra-thin diffusion boundary layer (DBL), similar to the behavior observed in heat transfer with high Prandtl numbers (Pr). Although it is uncommon to encounter applications with high Pr where the temperature field can still be treated as a passive scalar, we will not address such complexities in this paper. We assume that both mass and heat transfer can be treated as passive scalars, thereby ignoring the effects of variable density.

The direct coupling of these passive scalar transport phenomena with momentum transport is complex, mainly due to additional scaling that governs the micro-diffusive regime for passive scalar dynamics [4]. Resolving the viscous-diffusive regime requires a grid finer than the Kolmogorov scale for fluid turbulence. Consequently, modeling both fluid turbulence and passive scalar transport using the Eulerian approach remains challenging. Conducting Direct Numerical Simulation (DNS) for high Sc numbers is particularly difficult due to the exceedingly long representative time scales for passive scalars at very high Sc or Pr numbers. Therefore, high Sc or Pr number DNS is rare in the literature. Additionally, the limitations of available supercomputing resources and the challenges of handling and visualizing ultra-large computational grids make DNS for high Sc numbers infeasible for most research projects, with few exceptions among pioneering groups in turbulent flow research.

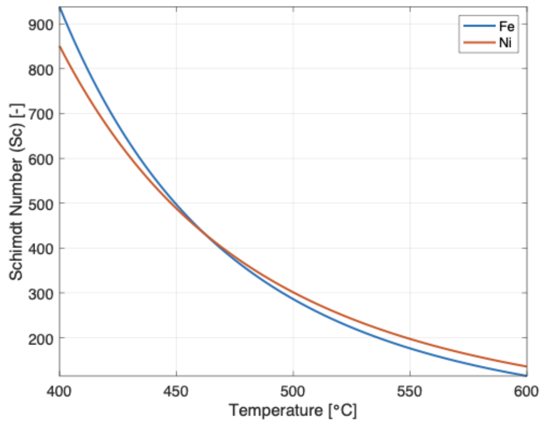

Figure 1: Schmidt number dependence for Fe and Ni in liquid lead.

In our modeling of the dissolution of structural materials in HLM, our primary focus is on obtaining a realistic estimate of the wall scalar flux to determine the dissolution and oxide removal rate. We prioritize this over delving into the micro-scale dynamics near the fluid-side boundary (i.e., we are not interested in the sub-grid scale micro-diffusive processes) due to the significant time-scale difference between the transport processes in the solid and fluid phases. Consequently, this study concentrates on an economical approach to modeling the near-wall diffusive flux in passive scalar transport for turbulent flows, particularly at high Sc or Pr numbers.

The objective of this research is to propose a model adjustment to enhance the capabilities of Wall-Modeled Reynolds-Averaged Navier-Stokes (WM-RANS) and Large Eddy Simulation (WM-LES) techniques in modeling passive scalar transport under conditions with high Sc or Pr numbers using a relatively coarse grid in passive scalar. For more background information on our research project on LFR and its implications for reactor applications, refer to our previous works in nuclear engineering publications [1, 5].

2 Need of Development of Modified Wall Model for High Schmidt or Prandtl Numbers Applications

In this section, we briefly discuss passive scalar physics at high Sc and evaluate the performance of widely adopted wall models in predicting passive scalar transport, comparing their results to existing LES and DNS data under Sc conditions (Table 1). Furthermore, we provide a literature survey for high frictional Reynolds number (Re_τ) conditions for completeness. However, since the studies at high Re_τ cover only low Sc ranges (Table 2), they are not used in our derivation for low-pass filtering effect. Consequently, the scarcity of high Re_τ LES or DNS data for high Sc ranges in the current literature highlights the need for further research in this area.

Table 1: Summary of mean profile data for low Re_τ ranges.

Re_τ	Pr/Sc Ranges	Method	Reference
180	[1, 3, 10, 25, 49]	DNS	[6]
150	[100, 200, 400]	DNS	[7]
360, 500	[1, 10, 20]	DNS	[8]
150	[0.025, 0.05, 0.1, 0.3, 1.0]	DNS	[9]
150	[1, 3, 10, 100, 500, 2400]	DNS	[10, 11]
180	[0.025, 0.05, 0.2, 0.4, 0.71, 1.0, 1.5, 5.0]	DNS	[12]
180, 395	[0.025, 0.2, 0.71]	DNS	[13]
180, 395	[0.71, 1, 2, 5, 7, 10]	DNS	[14]
150, 395	[100, 200, 500]	LES	[15]

Table 2: Summary of mean profile data for high Re_τ ranges.

Re_τ	Pr/Sc Ranges	Method	Reference
1140	[0.00625, 0.0125, 0.025, 0.0625, 0.125, 0.25, 0.5, 1, 2, 4, 16]	DNS	[16]
500, 1000, 2000	[0.007, 0.001, 0.002, 0.05, 0.01, 0.03, 0.5, 0.7]	DNS	[17]
500, 1000, 2000	[1, 2, 4, 7, 10]	DNS	[18]
Up to 6000	[1]	DNS	[19]
5000	[0.71]	DNS	[20]
500, 1000, 2000, 4000	[0.2, 0.71, 1]	DNS	[21]

2.1 Low-pass filtering phenomenon

At high Sc number, the concentration boundary layer (CBL) can be several hundred times thinner than the velocity boundary layer (VBL). The relative thickness of CBL with VBL can be approximated by the proportionality relation of $\mathrm{Sc}^{-0.333}$ [22], therefore, it would not be practical to refine the wall to resolve such small scale behaviour at $\mathrm{Sc} \rightarrow \mathrm{O}(10^2$ to $10^3)$ in scale-resolving simulation. Wall-resolved simulation can be adopted in time averaged turbulence simulation, however, extension to complex geometry remains difficult due to exceedingly wall refinement. An estimation of grid resolution was provided by [6] on passive scalar, which is:

$$\eta_B = \frac{\eta_K}{\sqrt{\mathrm{Sc}}}, \tag{1}$$

where η_B and η_K are the Batchelor and Kolmogorov length scales. The higher the Reynolds (Re) number, the more stringent would be the requirement to resolve the velocity fluctuations and the same holds true for small-scale passive scalar fluctuations.

When coupling of passive scalar transport under high Sc numbers in scale-resolving simulations, it is important to acknowledge that the time required to attain flow statistics equilibrium will also be influenced by Sc and in addition, the CFL time-step restriction due to much smaller mesh size. Achieving such equilibrium within a reasonable simulation time becomes unattainable in an Eulerian-based approach, let alone obtaining meaningful wall scalar flux statistics. Therefore, it is still rare to see coupled DNS and WRLES with high Sc number in open literature.

Given the elevated Sc number encountered in corrosion modelling, our goal is to utilize the same computational grid for velocity to effectively capture the near-wall passive scalar gradient. Therefore, it is crucial to evaluate the wall model, not only for its correctness concerning mean profiles but also for its accuracy in relation to the near-wall y^+ behaviour. An important aspect to consider when modelling passive scalar transport under high Sc or Pr conditions is the breakdown of Reynolds analogy between velocity and passive scalar fields. This breakdown is suggested by the distinct scaling relations observed in the turbulent energy spectrum, as mentioned earlier.

One notable characteristic of high Sc passive scalar transport is the significantly lower diffusiveness of the passive scalar field compared to the velocity field. This leads to different response timescales between the passive scalar and the velocity fields. Consider a fictional droplet with high diffusivity; in this scenario, any fluctuations resulting from turbulence mixing would be almost instantaneously responded to. Conversely, when the droplet possesses very low diffusivity, the response to such fluctuations will be comparatively diminished. In the extreme case, there may be no response at all.

It was demonstrated in [23] that for high Pr, the thermal perturbations induced by sliding bubbles in a laminar flow channel, requires a longer time to be reverted back to the laminar state than the velocity perturbations. This suggests that the perturbed temperature field remains in a temporary "frozen" state in comparison to the velocity perturbations, which decay rapidly in laminar flow. A similar analogy can be drawn regarding near-wall scalar fluctuations, where the time-lag effect in passive scalar fluctuations can significantly influence the behaviour of scalar eddy diffusivity in close proximity to the wall.

The time-lagging, or low-pass filtering effect, on scalar fluctuations in turbulent flows was investigated in [7] using spatial-temporal correlational analysis. This phenomenon, characterised by a delay in the response of scalar fluctuations, represents a nonlinear effect that cannot be accounted for in the typical derivation of asymptotic laws governing velocity and scalar eddy viscosity/diffusivity.

For passive scalar, one can express the dimensionless scalar gradient in the form of power series as performed routinely in boundary layer analysis [24]:

$$c'(y^+) = d_1 + d_2 y^+ + d_3 {y^+}^2 + d_4 {y^+}^3 + \cdots, \tag{2}$$

Using the fact of the second derivative of c' with respect to y^+ is zero [11], we have,

$$c'(y^+) = d_1 + d_3 {y^+}^2 + d_4 {y^+}^3 + \cdots, \tag{3}$$

It's crucial to acknowledge that not all fractional power functions possess a power series expansion, and such analyses provide no means to deduce non-integer exponents. This presents a challenge in passive scalar boundary analysis, particularly as DNS data indicate that the exponent for scalar eddy diffusivity near the wall is non-integer. Derivations relying on power series implicitly assume that the power exponent must be an integer. Consequently, this leads to the same conclusion as the velocity boundary analysis, yielding identical results Therefore, there is no possibility to deduce the resulting fractional exponent of $u'c'$ using this approach.

The conventional terminology, employing scaled diffusivity, primarily addresses the discrepancy in spatial diffusion characteristics of the field, yet overlooks temporal disparities. However, these discrepancies predominantly occur at small scales, particularly those in close proximity to the wall. In the current study, we assumed the conventional approach of scaled diffusivity remains applicable to flow mixing away from boundaries or in simulations where boundary effects are not critical. In addition, the focus on flow mixing in the bulk is of secondary importance for our intended application.

It should be emphasised that the low pass filtering effect is a physical phenomenon that should be considered when constructing a model of diffusive flux at high Sc or Pr numbers, and the deviation of conventional ${y^+}^3$ scaling is supported by several studies using experiment and numerical simulations [25, 10, 8, 7, 26, 15]. Disregarding this effect can result in errors in modelling assumptions of all scalar fluctuations are as responsive as the velocity perturbations with a scaled factor which is proportional to Sc or Pr.

2.2 Jayatilleke P-function

The passive scalar transport cannot be defined on a single scale, since $\alpha^+_{\mathrm{turb}} \propto {y^+}^3$. The variation of B_T is defined in terms of the Jayatilleke P-function [27] ($B_T = \mathrm{Pr}_t[B + P]$),

$$P = 9.24[{\mathrm{Pr}^*}^{3/4} - 1][1 + 0.28\exp(-0.007\mathrm{Pr}^*)] \tag{4}$$

where $\mathrm{Pr}^* = \mathrm{Pr}_t/\mathrm{Pr}$. The turbulent Pr number (Pr_t) is chosen as 0.85 in the official implementation from OpenFOAM version 2306. The disadvantage of the wall model is that it requires an empirical constant of Pr_t, which might not be applicable to a wide range of conditions, as demonstrated by [8] in the pipe flow DNS with high Pr number up to 20.

Figure 2 shows the comparison between the Jayatilleke P-function and literature DNS data. The Jayatilleke P-function performs well only in the logarithmic region and for relatively small Sc values. Consequently, it is not suitable for our intended application where Sc is on the order of hundreds.

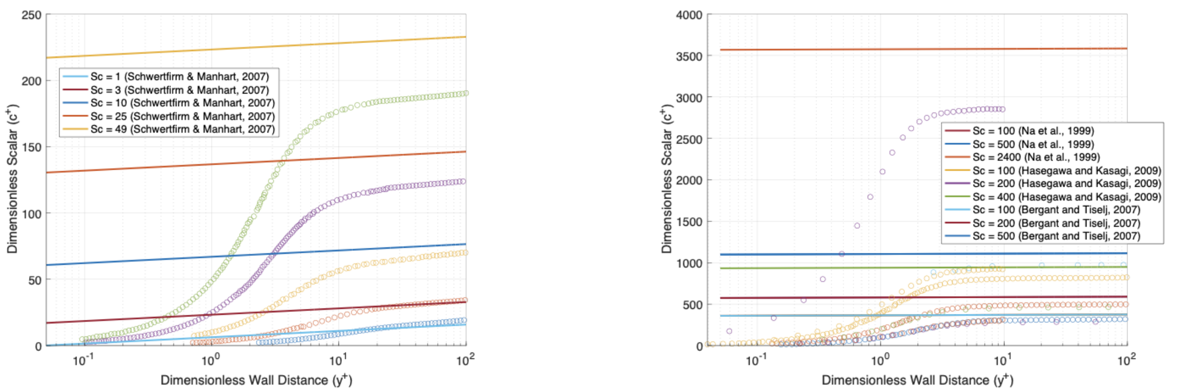

(a) Comparison between [27] wall model with literature data with Sc = 1-49 [6].

(b) Comparison between [27] wall model with literature data with Sc = 100-2400 [7, 15, 10].

Figure 2: Comparison between Jayatilleke [27] wall model and literature DNS data.

2.3 Kader's correlation

Kader [28] derived the following correlation for pipe and channel flow,

$$\theta^+ = \mathrm{Pr}y^+ \exp(-\Gamma) + \left[2.12 \ln\left((1+y^+)\frac{1.5(2-y/R)}{1+2(1-y/R)^2} + \beta(\mathrm{Pr})\right)\right] \exp(-1/\Gamma), \tag{5}$$

where R is the characteristic dimension of pipe or channel, Γ is,

$$\Gamma = \frac{10^{-2}(\mathrm{Pr}{y^+}^4)}{1+5\mathrm{Pr}^3 y^+}, \tag{6}$$

and β is calculated based on,

$$\beta(\mathrm{Pr}) = (3.85\mathrm{Pr}^{1/3} - 1.3)^2 + 2.12\ln(\mathrm{Pr}). \tag{7}$$

Figure 3 compares Kader's model with literature DNS data. Kader's model performs quite well over a wide range of Sc values; however, its accuracy diminishes at very large Sc values. Additionally, although Kader's model has the potential to be a universal y^+ wall model, the abrupt transition from the linear to the logarithmic region is somewhat unusual.

Although both Jayatilleke [27] and Kader [28] wall functions are frequently used in CFD software to model heat and mass transfer processes, new wall models should be developed to cover the application range of Sc where both existing models are not sufficiently accurate.

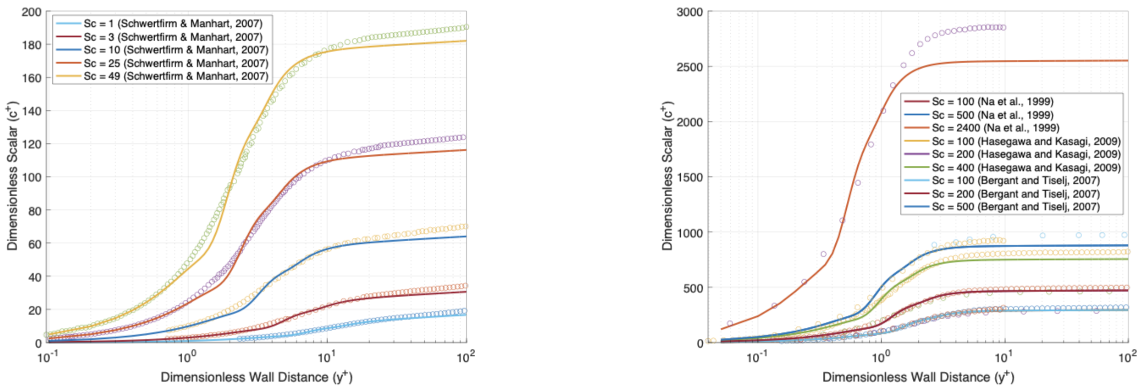

(a) Comparison between [28] wall model with literature data with Sc = 1-49 [6].

(b) Comparison between [28] wall model with literature data with Sc = 100-2400 [7, 15, 10].

Figure 3: Comparison between Kader [28] wall model and literature DNS data.

3 Wall Modeling with Modified Scalar Eddy Diffusivity

3.1 Assumption of the wall model and passive scalar phyiscs

To develop an enhanced wall model, there are a few physics aspects that the current available wall model fails to capture when dealing with turbulent flows at high Sc and Pr numbers.

1. The low-pass filtering effect of wall scalar fluctuations induces a deviation from the typical ${y^+}^3$ asymptotic behavior in scalar eddy diffusivity. This deviation is contrary to the expected trend based on analogy using eddy viscosity.

2. For passive scalar transport, it is required to consider the outer layer effect for smaller Sc (i.e., Sc>1). While this effect seems to be diminished when the Sc >> 1 [26].

3. Reynolds number effect on mean passive scalar profile is quite strong at $\mathrm{Re}_\tau < 500$, while its effect diminishes at higher Re_τ.

4. The higher the Sc, the higher the extent of the deviation from the conventional asymptotic scaling (${y^+}^3$ behavior). For Sc at extreme value, the gradient in the diffusivity would be very steep inside the $L_{\rm cond}$ (due to the reduction of $L_{\rm cond}$ with Sc). This would give an asymptotic zero wall scalar flux. [10] showed that the fractional exponent of α_t will change with Sc according to Lagrangian DNS data.

For precise modeling of near-wall diffusive flux, it is crucial to consider the low-pass filtering effect of the scalar field within the conductive layer. This effect manifests as a delay in responding to instantaneous perturbations induced by the velocity field. This discrepancy is the reason the conventional analogy with velocity proves inadequate. Therefore, a two-layer model was proposed (Figure 4),

1. The first layer contains the effect only due to passive scalar diffusive effects, where the hydrodynamic has limited effects, and also this is the region where low-pass filtering effect occurs.

2. The second layer is the routine viscous sub-layer for hydordynamic.

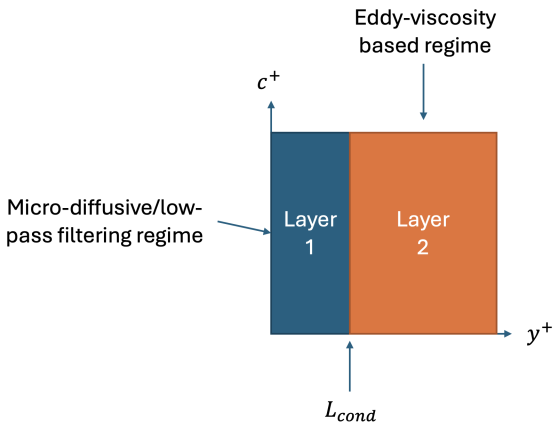

Figure 4: Conceptual schematic for the two-layer concept.

We propose to couple these two layer using the conductive boundary layer thickness (L_{cond}), which is available in [6],

$$L_{\rm cond} = 11.5 \cdot {\rm Sc}^{-0.29}. \tag{8}$$

The conductive layer thickness might have an dependence on the Re_τ, which can be observed by comparing [6] and [16] predictions. The correlation was derived the correlation based on the DNS data under a single frictional Re [6]. The current wall model does not account for the Re dependency of L_{cond} due to the lack of sufficient DNS data for high Re_τ with high Sc numbers in the existing literature. However, a similar correlation was also derived (with the numerical constant of 11.702 and -0.284) from [29] using [27] dataset, therefore, the validity of this equation is considered to be the state-of-the-art.

3.2 The two-layer numerical wall model

Existing algebraic wall models fail in obtaining adequate estimates of near-wall diffusive flux under such conditions due to the failure of velocity eddy viscosity analogy of $\alpha_t \to k{y^+}^3$ at $y^+ \to 0$ [30, 16],

$$\alpha^+(y^+) = \frac{(ky^+)^3}{C_{th}^2 + (ky)^2}. \tag{9}$$

The notation of the above formulation follows [16][1], where a term in the denominator has been omitted in compared to original form from [30]. However, it must be mentioned that alternative formulations exist to better capture the asymptotic behavior of the boundary layer, which can show better generalization; however, it is under our investigation, therefore, not reported in this conference paper. The idea of the

[1]It should be mentioned that, in [5], we also demonstrated that the wall model in this original form is not conforming to high Sc condition, due to the lack of high Sc data used in deriving such model. In addition, it is not possible to correct the Sc behaviour using single parameter based model.

current developed model is to propose improvement with minimal modification to improve the prediction of the wall model at high Sc or Pr numbers.

To reiterate, the objective of the model is to capture the variation of Re_τ and the Sc or Pr number for the k within the logarithmic region. Taking into account the physics of high Sc or Pr passive scalar transport, a more realistic approach involves incorporating a two-layer model, which consists of two regions governing by different k values, k_{Re} and k_{Sc}.

The fundamental assumption in constructing this two-layer model involves the complete decoupling of the effects from k_{Re} and k_{Sc}. In simpler terms, the isolation of Re_τ and Sc allows for the deduction of both constants independently. This provides a straightforward method to improve the current integral-type of wall model using the latest DNS databases, as illustrated in Tables 1 and 2.

We assume that the effect of Re and Sc can be decoupled, and this leads to two different values correlation (i.e., k_{Re} and k_{Sc}.) that can be used to improve our prediction using wall model. The two-layer model is based on [30], but by taking into account of the low-pass filtering behavior within the conductive layer using an indicator function to combine with conventional velocity scaling,

$$\alpha^+(y^+) = \frac{\beta k_{\mathrm{Re}} {y^+}^3 + (1-\beta) k_{\mathrm{Sc}} {y^+}^\alpha}{C_{th} + (k_{Re} y^+)^2} \tag{10}$$

The α is the exponent deviated from the ${y^+}^3$ scaling, which is taken as 3.3 in the current study. Alternative models can be derived using different β and α definitions; however, the spirit lies in the concept of two-layers and the decoupling of Re and Sc effects.

Even under current modification, the asymptotic behavior of the wall scaling is preserved at large y^+. Hence, this keeps the validity of such a model to be used in scale-resolving simulations, like LES. The indicator function β is calculated based on calculation of conductive layer thickness L_{cond},

$$\beta = \frac{1}{1 + \exp(y^+ - L_{\mathrm{cond}})}. \tag{11}$$

The choice of β is not unique and the current function of β is asymmetric upon closer inspection. The potential impact of this asymmetry will be discussed in the valuation section. In addition, the effect of the outer layer peaks is also very pronounce at low Sc numbers, therefore care must be taken to deduce the correct value for k_{Re}.

The proposed model is a numerical wall model (NWF), which takes y^+ and Re_τ as input to calculate the corresponding c^+ to deduce correction to the scalar turbulent diffusivity at the wall. One of the advantages of using this model is the elimination of dependency on the turbulent Prandtl number.

$$c^+(y^+, \mathrm{Re}_\tau) = \int_0^{y^+} \left[1 + \frac{y^+}{Re_\tau}\right] \frac{\mathrm{Sc}}{1 + \mathrm{Sc}\alpha^+}\, dy^+. \tag{12}$$

A modeling term for the outer layer peak (y^+/Re_τ) was added to the mean scalar transport equation. The formation of such outer layer peaks was not present in velocity field due to the presence of the pressure-strain redistribution in the momentum equation. The verification of such term to low Re_τ DNS is given in [5], therefore, is not repeated here. One benefit of using such a numerical wall model for both single-layer [16] and two-layer models is the elimination of the need to model the turbulent Prandtl number (Pr_t). This is due to its derivation based on a bottom-up scalar diffusivity approach, which leads to a complicated mathematical form in the derivation of wall models as seen in [8, 29, 27].

Figure 5 shows the verification of the two-layer model in comparison to the scalar eddy diffusivity of the DNS data in [16]. The success of the two-layer model and its agreement with the fractional exponent at $y^+ \to 0$ indicates that the consideration of low-pass filtering can be used to improve the prediction for $y^+ < L_{cond}$. The two-layer scalar diffusivity model better predicts the DNS data than the single-layer model with its original form ($k = 0.459$) and a fitted version ($k = 0.39$) which was still based on single layer model but attempted to fit the near-wall gradient in dimensionless scalar diffusivity, however, this would make the model deviates from the DNS data at larger y^+ value.

As hinted by the one-dimensional turbulence (ODT) model [26] and compared to several full-order DNS data, it can be seen that the value k is not a universal constant but a function of Re_τ. The strong influence of Re_τ and the effect of the outer layer on the wall scalar profile results in a poor prediction of the existing wall models in predicting passive scalar transport. An immediate extension of the wall model is to incorporate the transition behavior of k into the wall model.

With the use of the DNS database in the open literature (Table 1) for cases with Sc = 1, the

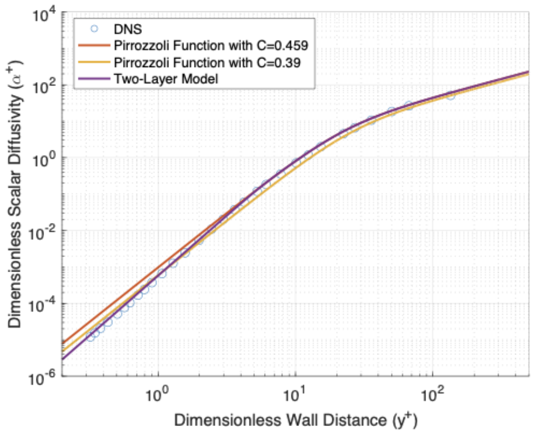

Figure 5: Dimensionless scalar diffusivity for DNS data of Pr=16 [16].

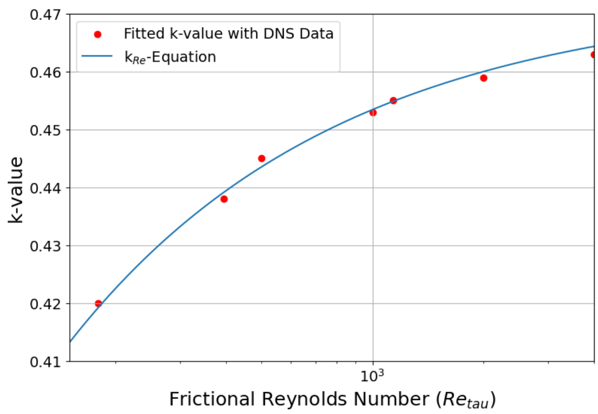

Figure 6: Variation of k_{Re} with respect to Re_τ

dependence of Re_τ on k_{Re} is deduced in Figure 6. The scatter data points are values of k that are the result of the best fitted curve against the integrated numerical wall profile, with the selected DNS mean scalar profile of Table 1 and 2.

The empirical relation of k_{Re} is assumed to be in the following form of the power law,

$$k_{\mathrm{Re}}(\mathrm{Re}_\tau) = a + b{\mathrm{Re}_\tau}^c \tag{13}$$

where $a = 0.473$, $b = -1.145$ and $c = -0.589$. The validity range of the k_{Re} empirical relation is in the Re_τ range between 150 to 6,000, with the use of DNS data of Sc=1 from [6, 14, 21, 19]. The increasing trend of k is similar to other previous research. Similarly, we deduced the k_{Sc} using the DNS data with various Sc under Re_τ of 150 and 180. The empirical relation of the k_{Sc} is assumed to be in the following form of power law,

$$k_{\mathrm{Sc}}(\mathrm{Sc}) = d + e\mathrm{Sc}^f \tag{14}$$

where $d = 0.425$, $e = -0.004$ and $f = 0.5$. The validity range of the k_{Sc} empirical relation is in the Sc range between 1 to 2,400 with the use of DNS data from [6, 7, 10, 11]. The reduction of k_{Sc} at high Sc is due to the reduction of the α^+ at y^+ very close to wall, in order to fit the increasing gradient within the L_{cond}, which also decrease with Sc. Additionally, it is observed that k_{Sc} remains relatively constant across the low Sc range (i.e., Sc < 50). While this observation might suggest the possibility of a two-region model, a single power law relation is employed for the sake of model robustness.

The complete implementation of the model in OpenFOAM for RANS and LES simulations, and the details of numerical integration test and the use of α_t correction formula are included in [5].

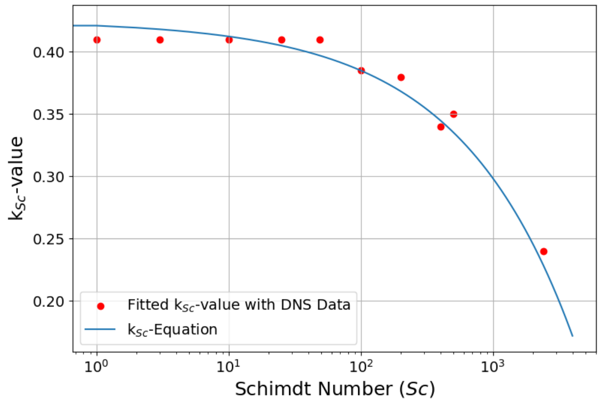

Figure 7: Variation of k_{Sc} with respect to Sc.

3.3 Verification of the two-layer model

Figure 8 shows the validation of the current two-layer model against DNS data at lower Re_τ, demonstrating favourable agreement between the model and these low Re_τ DNS datasets. Figure 9 presents the comparison between the numerical predictions of the wall model and the LES results provided in [15]. Although not used to derive the correlation factors, numerical predictions produce reasonable alignment with LES data at higher Re_τ (for the case with Sc = 100 and 200, which were at Re_τ=395). Figure 10 shows the comparison between the numerical wall model with the same set of data but using the conductive boundary layer equation that was empirically derived based on the approximated solution from [16],

$$L_{cond} = 10.5\ \mathrm{Sc}^{-0.33}. \tag{15}$$

The refined correlation, established for high Re_τ conditions, has the potential to improve predictions for cases with Sc = 100 and 200. However, due to the narrow range of Pr numbers in the DNS utilized for model validation and the better general agreement to the cases in Figure 9 in terms of the non-normalized scalar value (c^+), we opted to continue using the conductive boundary layer equation by [6] in subsequent analyzes. It should be noted that, due to the independent derivation of the Sc and Re-dependent factors, the developed correlation for both k_{Re} and k_{Sc}, can be adapted to various conductive layer equations.

Given the scarcity of higher Re_τ data, we turn to Sc = 1 DNS data [21] for comparison with the predictions of the numerical wall model, as illustrated in Figure 11. The numerical wall model demonstrates good agreement across the Re_τ range from 500 to 4000 and captures the minor transition in slope within the logarithmic layer with respect to increasing Re_τ.

The numerical wall model demonstrates reasonable agreement in predicting the mean scalar profile when compared with available DNS and LES data. Future refinements can be anticipated with the availability of DNS data under high Sc and high Re_τ conditions. These verification tests underscore the capability of the two-layer wall model to provide a reasonable estimation of the wall scalar mean profile through independently derived correlation factors that isolate the effects of Re and Sc.

4 Validation with High Sc Mass Transfer Pipe Experiments

In this section, we present the performance of combining the proposed wall model with several wall refinements at $y^+ = 1$ (wall-resolved) and larger y^+ (wall-modeled). We simulate a turbulent pipe flow with a diameter of D_h and a length of $100D_h$ to ensure fully developed flow conditions. The wall scalar flux is taken from the fully developed flow condition and averaged over the circumference of the wall. The required first cell thickness is calculated using the desired y^+, D_h, and mean velocity (U_m). Depending on the first wall thickness, 15-20 prism cells are imposed on the wall.

The open-source CFD software, OpenFOAM version 2306, was used to conduct these simulations with the kOmegaSST model. We believe that for such a simple geometry, the kOmegaSST model suffices for the application. The turbulent Schmidt number (Sc_t) is set as 0.9 due to very weak feedback to large scale dynamics in high Sc flows. Furthermore, the current simulation is merely a case for demonstrating the capability of the two-layer model. The two-layer model is implemented as a new boundary condition for α_t using Boost's numerical integration capability (i.e., adaptive Gauss-Kronrod quadrature) already

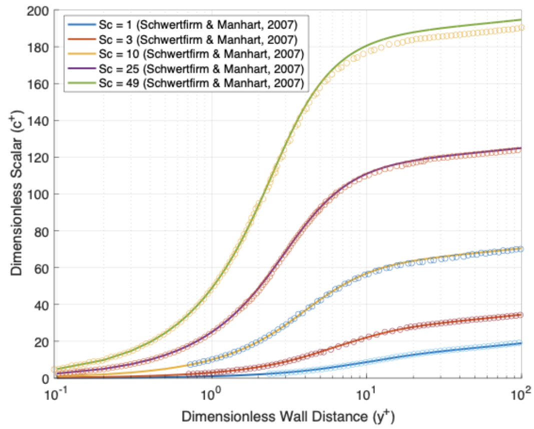

(a) Comparison between wall model with literature data with Sc = 1-49 [6].

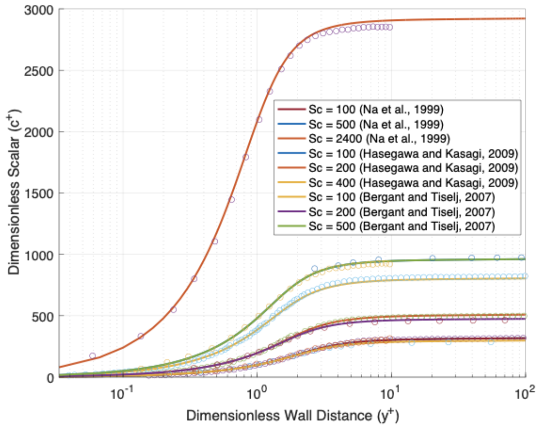

(b) Comparison between wall model with literature data with Sc = 100-2400 [7, 15, 10, 11].

Figure 8: Comparison between two-layer wall model and literature DNS data. The legend describes the prediction made by the two-layer model for the respective scenario in the literature.

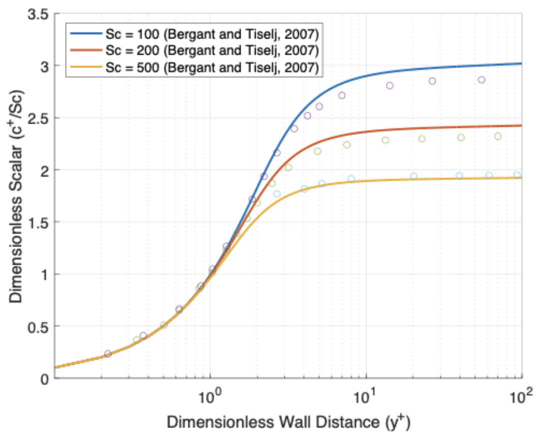

Figure 9: Verification of numerical wall model with LES mean profile from 100 to 500 [15] with $L_{cond} = 11.5\ \mathrm{Sc}^{-0.29}$.

installed in the standard configuration of OpenFOAM. In [5], we analyzed the use of different integration techniques for the wall model, and the adaptive Gauss-Kronrod quadrature approach was found to have

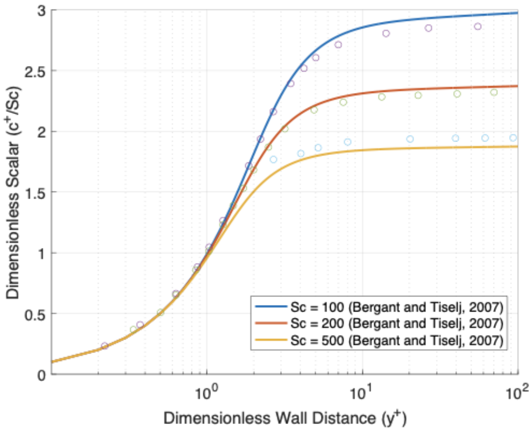

Figure 10: Verification of numerical wall model with LES mean profile from 100 to 500 [15] with $L_{cond} = 10.5\ \mathrm{Sc}^{-0.34}$.

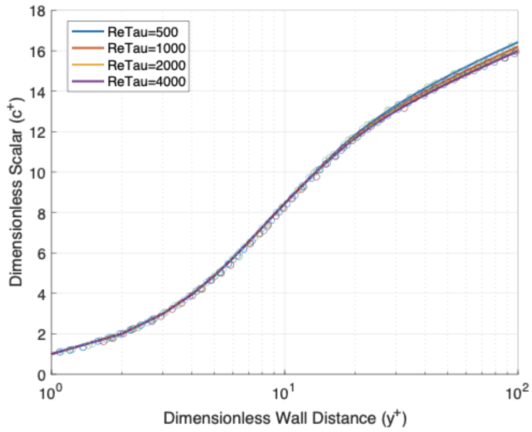

Figure 11: Verification of numerical wall model with high Re_τ DNS at $\mathrm{Sc} = 1$ [21]

the best cost-to-performance ratio; therefore, it was adopted in our two-layer model.

The boundary conditions for the wall-resolved and wall-modeled simulations are detailed in Table 3 and 4. The primary distinction lies in the application of wall functions/models to the k and ν_t. Wall models are applied to α_t and ω for wall-resolved and wall-modeled simulations.

	Inlet	Outlet	Wall
p	zeroGradient	fixedValue	zeroGradient
U	codedFixedValue	zeroGradient	noSlip
c	fixedValue	zeroGradient	fixedValue
k	turbulentIntensityKineticEnergyInlet	zeroGradient	fixedValue
ω	calculated	zeroGradient	OmegaWallFunction
ν_t	calculated	zeroGradient	fixedValue
α_t	calculated	zeroGradient	TwoLayerWalModel

Table 3: Boundary conditions for $y^+ = 1$ simulation.

The coupling of the wall-resolved hydrodynamic simulation with a wall model for α_t is justified by the need to accurately capture a highly underresolved passive scalar field. Under high Sc conditions, accurately capturing the scalar gradient requires using a grid with y^+ smaller than 0.1, as reported in [31] for Sc=1000. Only at such small y^+ values does turbulent mass transport become negligible, comparable to molecular diffusive transport. Therefore, we are interested in two modeling scenarios:

1. Simulating the hydrodynamics with high accuracy using a wall-refined grid (down to y^+ close

	Inlet	Outlet	Wall
p	zeroGradient	fixedValue	zeroGradient
U	codedFixedValue	zeroGradient	noSlip
c	fixedValue	zeroGradient	fixedValue
k	turbulentIntensityKineticEnergyInlet	zeroGradient	kqRWallFunction
ω	fixedValue	zeroGradient	OmegaWallFunction
ν_t	calculated	zeroGradient	nutSpaldingsWallFunction
α_t	calculated	zeroGradient	TwoLayerWalModel

Table 4: Boundary conditions for $y^+ = 15$ simulation.

to 1) and modeling the under-resolved passive scalar field with a two-layer model. (Combining wall-resolved and wall-modeled simulations)

2. Simulating both hydrodynamics and the passive scalar using wall models. (Coarse grid simulations and the basis for coupling both fields in wall-modeled LES)

We will not delve into wall-modeled LES in this paper due to the lack of a clear validation basis for common instantaneous time characteristics. The wall model approach has been verified in the previous section, demonstrating its conformity with a wide range of DNS/LES mean profiles. However, it is possible to compare time-averaged predictions (from RANS) with high Sc mass transfer experiments from both [15, 25] In [32], high Sc mass transfer pipe experiment was conducted in electrochemical system by measuring the concentration difference in the pipe flow, and given the following correlation,

$$St_d = 0.0165\mathrm{Re}^{-0.14}\mathrm{Sc}^{-0.67}, \tag{16}$$

with a validity range for Sc between 1000 to 6000 and Re between 8×10^3 to 2×10^5. In [25], asymptotic correlation were derived based on theoretical analysis and high Sc experiment up to O(10^4),

$$K_v = 0.0889v^*\mathrm{Sc}^{-0.704}, \tag{17}$$

where v^* is frictional velocity, and the correlation is an asymptotic correlation for very large Sc. To convert these correlations to the wall scalar flux, we also used the following frictional factor correlation for pipe,

$$f = \frac{1}{[1.8log(\mathrm{Re}) - 1.5]^2}, \tag{18}$$

and the usual description of mass transfer coefficient.

These two correlations are regarded the gold standard for high Sc simulations, as evidenced by previous RANS and LES studies in the open literature. In this study, we limit the validation exercise to a Re number of 400,000, as this is the upper limit for the correlations presented thus far. Although the wall model can predict high Re, we anticipate that the changes at high Re are minimal compared to the behavior at low Re. Additionally, due to the lack of reliable validation data at the time of writing, high Re cases have been excluded from the current work.

4.1 Mesh sensitivity in conforming to mean profile

Before discussing the results compared to the mass transfer rate, we present the mesh sensitivity with respect to y^+ in relation to the applied mean profile. Figure 12 illustrates the variation in the scalar-centered value with respect to the first grid resolution. The mean profiles are well-conformed for smaller y^+ values but tend to deviate slightly at very high y^+ values. In general, the two-layer model is not sensitive to the choice of y^+ in this test.

4.2 Wall scalar flux predictions with Sc=1000, 500, 250

Our aim is to evaluate the performance of the model in relation to established experiment mass transfer result. It is essential to clarify that our study does not seek to conclusively establish the superiority of either a bottom-up approach, such as the two-layer model, or experimental correlations in predicting wall scalar flux in this test case. To accomplish this goal, we would need more dedicated experiments conducted at high Re numbers and high Sc numbers, which are regrettably scarce in the current open

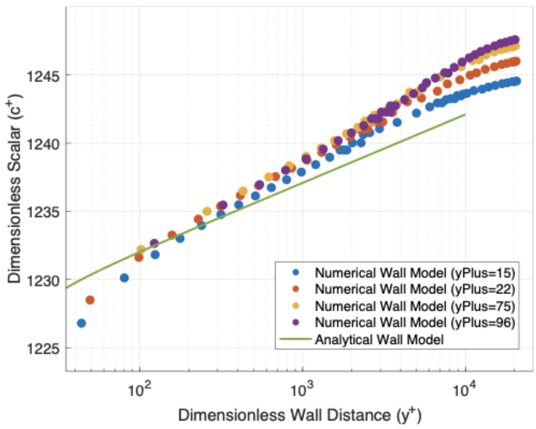

Figure 12: Conformance with y^+ on imposed wall model.

literature. Consequently, the validation of such flow cases will remain a subject for future investigations. Instead, we offer predictions derived from the numerical wall model and compare them with existing correlations. In doing so, we provide practitioners interested in adopting the current wall model with insights into its predictive capabilities, aiding them in making informed decisions regarding whether to adopt the two-layer model or conventional single-layer wall model [16] or empirical models such as [27, 28].

We first performed a simulation with Sc = 1000, as shown in Figure 13, across a range of y^+ values. For high y^+, the CFD predictions agree well with both correlations [15, 25], recommending its use for high Sc mass transfer applications without the need for highly refined meshes. However, we observed a deterioration in performance at smaller y^+ values, starting at $y^+ = 1.5$ and worsening to $y^+ = 0.5$, which might not be optimal for combining the wall model with the wall-refined hydrodynamic grid.

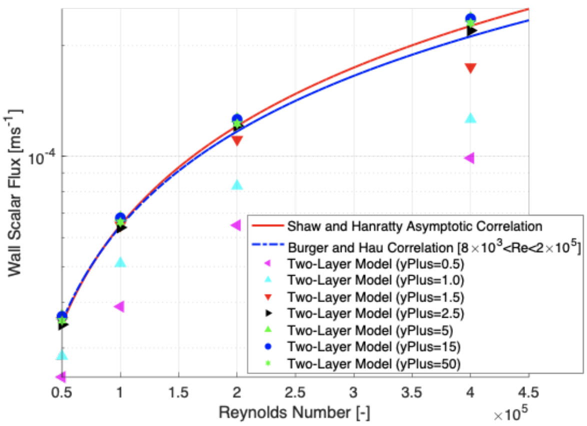

Figure 13: Wall scalar flux prediction with comparison to high Sc mass transfer experiment [15, 25] at Sc=1000.

From our numerical predictions at Sc = 1000, we identified that if the first grid resolution is at $y^+ = 1.5$ or lower, the wall scalar flux will be quite poor. We hypothesize that this error is due to the correction lying within the first layer of our model; this can be linked to the asymmetric nature of the indicator function (β). Routine application of wall model within such region leads to error in wall scalar flux. To verify such claim, we performed two additional simulations with Sc = 500 and Sc = 250, both with larger L_{cond} values than the case with Sc = 1000, which are approximately 1.9 and 2.3, respectively.

From Figures 14 and 15, we observe that precision decreases at $y^+ = 1.5$, which is similar to the case for Sc = 1000. This suggests that the minimum y^+ at which the wall model maintains its accuracy appears to be independent of the Sc number. A similar trend of deviation is observed at higher Re numbers.

We believe that this is due to the β formulation, which is more skewed on the side with negative

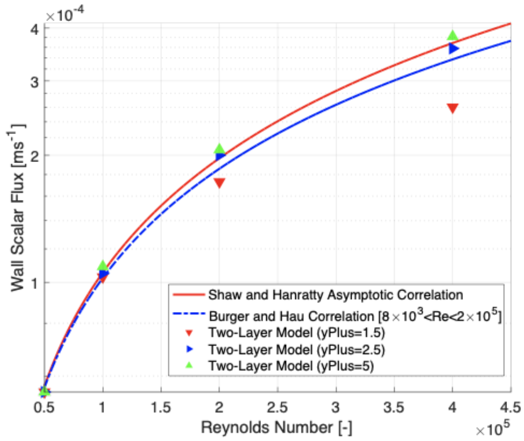

Figure 14: Wall scalar flux prediction with comparison to high Sc mass transfer experiment [15, 25] at Sc=500.

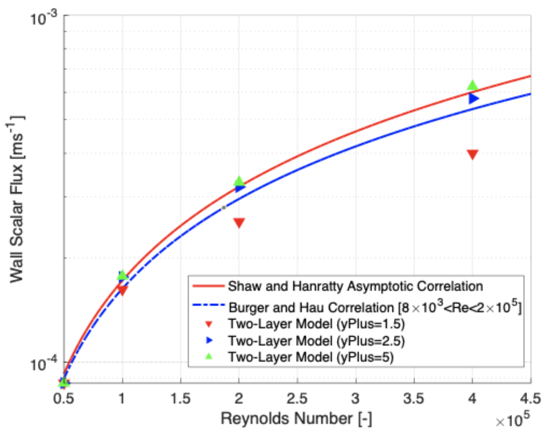

Figure 15: Wall scalar flux prediction with comparison to high Sc mass transfer experiment [15, 25] at Sc=250.

$y^+ - L_{cond}$ (Figure 16). A much larger transition region appears on the negative side. Therefore, the "unphysical" behavior introduced by the indicator function feeds more into layer 1 instead of layer 2.

A better alternative for a symmetric indicator function β_2 is proposed as,

$$\beta_2 = 1 - \frac{1}{2}\left[1 + \tanh\left(\frac{y^+ - L_{cond}}{A}\right)\right], \tag{19}$$

where A is the transition region thickness. With the use of hyperbolic tangent function, we can control both the transition thickness[2] and have a symmetric indicator function (Figure 17). This is currently under our investigation. However, the high Re deviation at $y^+ = 1.5$ indicates that this behavior is related to the Re number, which requires further analysis.

For optimal accuracy with wall-resolved hydrodynamic results, it is essential to ensure that the coupling point for the wall model is outside of L_{cond} and much larger than 2.5 as demonstrated in the above analysis. This does not mean that the choice of the first grid y^+ should be restricted by this arrangement, as one can choose the second off-wall cell instead of the first as the coupling point to avoid this issue. We observe a similar requirement for WM-LES in hydrodynamics, where the use of the first off-wall cell causes significant error compared to using the second or third off-wall cells. However, the origin of this error might be different; nonetheless, it is not a critical issue in terms of wall modeling. In certain flow conditions, such as flow across an orifice or recirculating flow, accurate modeling of such effects cannot be achieved with a coarse grid for hydrodynamics alone, making the combined use of a

[2] which cannot be done in the current form of β

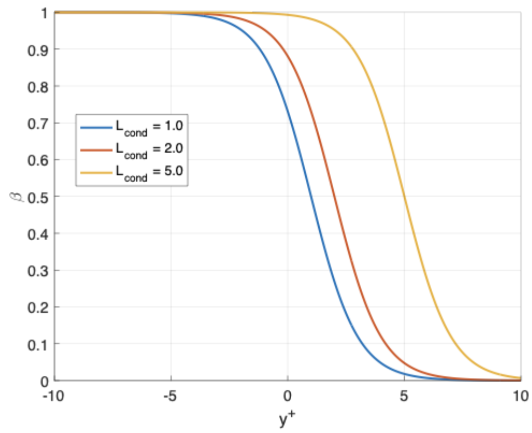

Figure 16: β indicator function

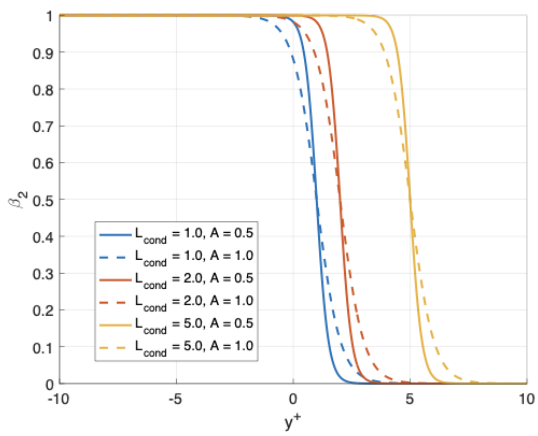

Figure 17: β_2 indicator function

wall-resolved hydrodynamic grid and a coarse grid for passive scalars inevitable.

5 Conclusion and Future Work

We have introduced an economical two-layer model for passive scalar transport that decouples the effects of Sc and Re, enhancing the prediction of near-wall diffusive flux. This model benefits both RANS and WMLES applications for high Sc conditions. The predictions of the wall model align well with existing DNS and LES mean profiles available in the literature. The wall-modeled RANS provides wall scalar flux predictions in good agreement with the mass transfer experiments by [32, 25]. The numerical model is designed to be easily implemented within conventional CFD frameworks. It can be applied to coupled coarse grid simulations for hydrodynamics and passive scalars, or to coarse grid passive scalar and refined grid hydrodynamic simulations.

With the use of the asymmetric indicator function (β), the minimum coupling point y^+ must be carefully chosen to achieve optimal accuracy. In this study, we focus on simulations up to a Re of 400,000, which covers a wide range of industrial flows. It is possible that the accuracy may deteriorate at even higher Re values with the current safe choice of the y^+ coupling point. Therefore, further studies will be conducted at higher Re numbers for this specific form of β. This is particularly relevant to our SEFACE facility [1], which covers a wide range of Re numbers in the millions.

We also propose an alternative form of the symmetric hyperbolic tangent indicator function β_2, which is currently under investigation to further reduce the effect of transition region on the diffusive layer (layer 1). Future work will include more challenging test cases involving orifices and recirculation to complete the validation of coupled coarse grid and wall-refined grid simulations to complete the two-layer model development for smooth surface. In the long term, we plan to incorporate roughness effects into the current wall model.

Acknowledgments

Current research is supported by the Swedish Foundation for Strategic Research (SSF) through Grant No. ARC19-0043 granted to the Sustainable Nuclear Energy Research in Sweden (SUNRISE) project. The computations were enabled by resources provided by the National Academic Infrastructure for Supercomputing in Sweden (NAISS) and the Swedish National Infrastructure for Computing (SNIC) at Tetralith HPC cluster, National Supercomputer Centre (NSC), which were partially funded by the Swedish Research Council through grant agreements no. 2022-06725 and no. 2018-05973.

References

[1] Kin Wing Wong, Ignas Mickus, Nathaniel Torkelson, Sumathi Vasudevan, Haipeng Li, Dmitry Grishchenko, and Pavel Kudinov. Hydrodynamic design of the Separate Effect test facility for Flow-Accelerated Corrosion and Erosion (SEFACE) studies in liquid lead. *Nuclear Engineering and Design*, 417:112852, February 2024.

[2] OECD and Nuclear Energy Agency. *Handbook on Lead-bismuth Eutectic Alloy and Lead Properties, Materials Compatibility, Thermalhydraulics and Technologies*. Nuclear Science. OECD, November 2015.

[3] Yun Gao, Minoru Takahashi, and Masao Nomura. Experimental study on diffusion of ni in lead-bismuth eutectic (lbe). *Energy Procedia*, 71:313–319, 2015.

[4] Hendrik Tennekes and John Leask Lumley. *A first course in turbulence*. MIT press, 1972.

[5] Kin Wing Wong, Ignas Mickus, Dmitry Grishchenko, and Pavel Kudinov. Enabling passive scalar wall modelling in large eddy simulation for turbulent flows at high schmidt or prandtl numbers. In *International Conference in Nuclear Engineering (ICONE-31)*, Prague, Czech Republic, 2024. Accepted.

[6] Florian Schwertfirm and Michael Manhart. DNS of passive scalar transport in turbulent channel flow at high Schmidt numbers. *International Journal of Heat and Fluid Flow*, 28(6):1204–1214, December 2007.

[7] Yosuke Hasegawa and Nobuhide Kasagi. Low-pass filtering effects of viscous sublayer on high Schmidt number mass transfer close to a solid wall. *International Journal of Heat and Fluid Flow*, 30(3):525–533, June 2009.

[8] C. Irrenfried and H. Steiner. DNS based analytical P-function model for RANS with heat transfer at high Prandtl numbers. *International Journal of Heat and Fluid Flow*, 66:217–225, August 2017.

[9] Marzio Piller, Enrico Nobile, and Thomas J. Hanratty. DNS study of turbulent transport at low Prandtl numbers in a channel flow. *Journal of Fluid Mechanics*, 458:419–441, May 2002.

[10] Yang Na, Dimitrios V Papavassiliou, and Thomas J Hanratty. Use of direct numerical simulation to study the effect of Prandtl number on temperature fields. 1999.

[11] Y. Na and T.J. Hanratty. Limiting behavior of turbulent scalar transport close to a wall. *International Journal of Heat and Mass Transfer*, 43(10):1749–1758, May 2000.

[12] Hiroshi Kawamura, Kouichi Ohsaka, Hiroyuki Abe, and Kiyoshi Yamamoto. DNS of turbulent heat transfer in channel flow with low to medium-high Prandtl number fluid. 1998.

[13] Hiroshi Kawamura, Hiroyuki Abe, and Yuichi Matsuo. DNS of turbulent heat transfer in channel flow with respect to Reynolds and Prandtl number effects. 1999.

[14] Makoto Kozuka, Yohji Seki, and Hiroshi Kawamura. DNS of turbulent heat transfer in a channel flow with a high spatial resolution. *International Journal of Heat and Fluid Flow*, 30(3):514–524, June 2009.

[15] Robert Bergant and Iztok Tiselj. Near-wall passive scalar transport at high Prandtl numbers. *Physics of Fluids*, 19(6):065105, June 2007.

[16] Sergio Pirozzoli. An explicit representation for mean profiles and fluxes in forced passive scalar convection. *Journal of Fluid Mechanics*, 968:R1, 2023.

[17] F. Alcántara-Ávila, S. Hoyas, and M.J. Pérez-Quiles. DNS of thermal channel flow up to Re τ = 2000 for medium to low Prandtl numbers. *International Journal of Heat and Mass Transfer*, 127:349–361, December 2018.

[18] F. Alcántara-Ávila and S. Hoyas. Direct numerical simulation of thermal channel flow for medium–high Prandtl numbers up to Re$\tau = 2000$. *International Journal of Heat and Mass Transfer*, 176:121412, September 2021.

[19] Sergio Pirozzoli, Joshua Romero, Massimiliano Fatica, Roberto Verzicco, and Paolo Orlandi. DNS of passive scalars in turbulent pipe flow. *Journal of Fluid Mechanics*, 940:A45, June 2022.

[20] Francisco Alcántara-Ávila, Sergio Hoyas, and María Jezabel Pérez-Quiles. Direct numerical simulation of thermal channel flow for and Re$\tau = 5000$ and Pr = 0.71. *Journal of Fluid Mechanics*, 916:A29, June 2021.

[21] Sergio Pirozzoli, Matteo Bernardini, and Paolo Orlandi. Passive scalars in turbulent channel flow at high Reynolds number. *Journal of Fluid Mechanics*, 788:614–639, February 2016.

[22] S Nešiĉ and J Postlethwaite. Hydrodynamics of disturbed flow and erosion—corrosion. part i—single-phase flow study. *The Canadian Journal of Chemical Engineering*, 69(3):698–703, 1991.

[23] KW Wong, L Bures, and K Mikityuk. Interface tracking investigation of the sliding bubbles effects on heat transfer in the laminar regime. *Nuclear Technology*, 208(8):1266–1278, 2022.

[24] Michael Leschziner. *Statistical turbulence modelling for fluid dynamics-demystified: an introductory text for graduate engineering students.* World Scientific, 2015.

[25] Dudley A Shaw and Thomas J Hanratty. Turbulent mass transfer rates to a wall for large schmidt numbers. *AIChE Journal*, 23(1):28–37, 1977.

[26] Marten Klein, Heiko Schmidt, and David O. Lignell. Stochastic modeling of surface scalar-flux fluctuations in turbulent channel flow using one-dimensional turbulence. *International Journal of Heat and Fluid Flow*, 93:108889, February 2022.

[27] Chandra Laksham Vaidyaratna Jayatilleke. The influence of prandtl number and surface roughness on the resistance of the laminar sub-layer to momentum and heat transfer. 1966.

[28] B.A. Kader. Temperature and concentration profiles in fully turbulent boundary layers. *International Journal of Heat and Mass Transfer*, 24(9):1541–1544, September 1981.

[29] Sanjin Saric, Andreas Ennemoser, Branislav Basara, Heinz Petutschnig, Christoph Irrenfried, Helfried Steiner, and Günter Brenn. Improved modeling of near-wall heat transport for cooling of electric and hybrid powertrain components by high prandtl number flow. *SAE International Journal of Engines*, 10(3):778–784, 2017.

[30] Antony J Musker. Explicit expression for the smooth wall velocity distribution in a turbulent boundary layer. *AIAA Journal*, 17(6):655–657, 1979.

[31] S Nešić, J Postlethwaite, and DJ Bergstrom. Calculation of wall-mass transfer rates in separated aqueous flow using a low reynolds number κ-ε model. *International journal of heat and mass transfer*, 35(8):1977–1985, 1992.

[32] FP Berger and K-FF-L Hau. Mass transfer in turbulent pipe flow measured by the electrochemical method. *International Journal of Heat and Mass Transfer*, 20(11):1185–1194, 1977.